

May 2007

# Crystal Structure of Formate Dehydrogenase H: Catalysis Involving Mo, Molybdopterin, Selenocysteine, and an Fe<sub>4</sub>S<sub>4</sub> Cluster

Jeffrey C. Boyington  
*National Institutes of Health (NIH), Rockville, MD*

Vadim Gladyshev  
*University of Nebraska - Lincoln, vgladyshev1@unl.edu*

Sergei V. Khangulov  
*Princeton University, Princeton, NJ*

Thressa C. Stadtman  
*National Institutes of Health (NIH), Rockville, MD*

Peter D. Sun  
*National Institutes of Health (NIH), Rockville, MD*

Follow this and additional works at: <http://digitalcommons.unl.edu/biochemgladyshev>

 Part of the [Biochemistry, Biophysics, and Structural Biology Commons](#)

---

Boyington, Jeffrey C.; Gladyshev, Vadim; Khangulov, Sergei V.; Stadtman, Thressa C.; and Sun, Peter D., "Crystal Structure of Formate Dehydrogenase H: Catalysis Involving Mo, Molybdopterin, Selenocysteine, and an Fe<sub>4</sub>S<sub>4</sub> Cluster" (2007). *Vadim Gladyshev Publications*. 29.

<http://digitalcommons.unl.edu/biochemgladyshev/29>

This Article is brought to you for free and open access by the Biochemistry, Department of at DigitalCommons@University of Nebraska - Lincoln. It has been accepted for inclusion in Vadim Gladyshev Publications by an authorized administrator of DigitalCommons@University of Nebraska - Lincoln.

# Crystal Structure of Formate Dehydrogenase H: Catalysis Involving Mo, Molybdopterin, Selenocysteine, and an Fe<sub>4</sub>S<sub>4</sub> Cluster

Jeffrey C. Boyington, Vadim N. Gladyshev,\*  
Sergei V. Khangulov, Thressa C. Stadtman, Peter D. Sun†

Formate dehydrogenase H from *Escherichia coli* contains selenocysteine (SeCys), molybdenum, two molybdopterin guanine dinucleotide (MGD) cofactors, and an Fe<sub>4</sub>S<sub>4</sub> cluster at the active site and catalyzes the two-electron oxidation of formate to carbon dioxide. The crystal structures of the oxidized [Mo(VI), Fe<sub>4</sub>S<sub>4(ox)</sub>] form of formate dehydrogenase H (with and without bound inhibitor) and the reduced [Mo(IV), Fe<sub>4</sub>S<sub>4(red)</sub>] form have been determined, revealing a four-domain αβ structure with the molybdenum directly coordinated to selenium and both MGD cofactors. These structures suggest a reaction mechanism that directly involves SeCys<sup>140</sup> and His<sup>141</sup> in proton abstraction and the molybdenum, molybdopterin, Lys<sup>44</sup>, and the Fe<sub>4</sub>S<sub>4</sub> cluster in electron transfer.

Formate dehydrogenase H (FDH<sub>H</sub>), a 79-kD polypeptide that oxidizes formate to carbon dioxide with the release of a proton and two electrons, is a component of the anaerobic formate hydrogen lyase complex of *E. coli* (1). Essential to its catalytic activity are an Fe<sub>4</sub>S<sub>4</sub> cluster, a Mo atom that is coordinated by two MGD cofactors, and a SeCys residue (2–4). With the recent determination of the crystal structures of three other molybdopterin (MPT)–containing enzymes (5–8), a functional role for the Mo-MPT cofactor has begun to emerge. However, the precise role of the active site selenium in this type of selenoenzyme and its interaction with Mo-MPT cofactors and the Fe<sub>4</sub>S<sub>4</sub> cluster remains to be elucidated (9).

The structure of *E. coli* FDH<sub>H</sub>, as solved by multiple isomorphous replacement (MIR) and multiwavelength anomalous dispersion (MAD) methods (Table 1), consists of four αβ domains (Fig. 1). The first domain (residues 1 to 60, 448 to 476, and 499 to 540), comprising two small antiparallel β sheets and four helices, coordinates the Fe<sub>4</sub>S<sub>4</sub> cluster just below the protein surface. The MGD-binding domains II (residues 61 to 135, 336 to 447, and 477 to 498) and III (residues 136 to 335) are each αβ sandwiches with overall topologies that closely resemble the classical dinucleotide-binding fold (10). A marked twofold pseudosymmetry is observed relating the cen-

tral portions of domains II and III. Despite their low sequence homology (<20% identity), the two domains can be superimposed to a root-mean-square (rms) deviation of 1.2 Å for 56 α carbons. SeCys<sup>140</sup>, an essential ligand to Mo, is located in a short loop at the NH<sub>2</sub>-terminus of domain III. The COOH-terminal domain (residues 541 to 715) consists of a

six-stranded mixed β barrel and five helices.

Similar to the active sites observed in aldehyde ferredoxin oxidoreductase and dimethyl sulfoxide (DMSO) reductase, the active site Mo of FDH<sub>H</sub> is coordinated by two tightly bound MGD cofactors, each containing a tricyclic ring system with a pyran ring fused to the pterin (6, 7). The Mo di(MGD) of FDH<sub>H</sub> is ligated within the interfaces of all four domains through an extensive network of hydrogen bonds, salt bridges, and van der Waals interactions, most of which involve domains II, III, and IV (Fig. 2). Domain II exclusively coordinates MGD<sup>801</sup> while domain III coordinates MGD<sup>802</sup>. Domain IV forms a cap over the bound pterin cofactors as it straddles domains II and III. Of the 35 residues that coordinate the Mo di(MGD) cofactor through hydrogen bonds, 23 are well conserved among the known MGD-containing formate dehydrogenases (11); the remaining 12 residues interact primarily through main chain hydrogen bonds (Fig. 2).

In both the reduced Mo(IV) and oxidized Mo(VI) structures, Mo is ligated to the four cis-dithiolene sulfurs of the MGD cofactors and the selenium of SeCys<sup>140</sup>. The coordination geometry of Mo in formate-reduced FDH<sub>H</sub> is closely approximated by a square

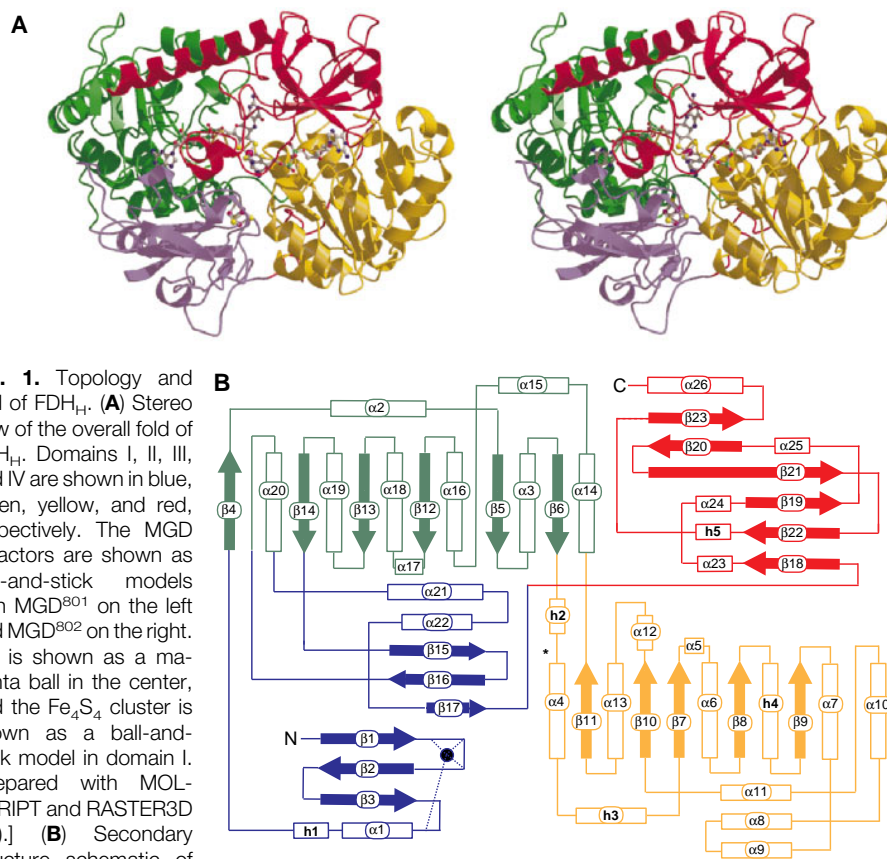


**Fig. 1.** Topology and fold of FDH<sub>H</sub>. (A) Stereo view of the overall fold of FDH<sub>H</sub>. Domains I, II, III, and IV are shown in blue, green, yellow, and red, respectively. The MGD cofactors are shown as ball-and-stick models with MGD<sup>801</sup> on the left and MGD<sup>802</sup> on the right. Mo is shown as a magenta ball in the center, and the Fe<sub>4</sub>S<sub>4</sub> cluster is shown as a ball-and-stick model in domain I. [Prepared with MOLSCRIPT and RASTER3D (26).] (B) Secondary structure schematic of FDH<sub>H</sub>. Domains I to IV are color-coded as in (A); α helices are numbered from α1 to α26, 3<sub>10</sub> helices are numbered from h1 to h4, and β strands are numbered from β1 to β23. The location of SeCys<sup>140</sup> is denoted by an asterisk; the location of the Fe<sub>4</sub>S<sub>4</sub> cluster is denoted by a solid blue circle.

J. C. Boyington and P. D. Sun, Structural Biology Section, Laboratory of Molecular Structure, National Institute of Allergy and Infectious Diseases, National Institutes of Health (NIH), 12441 Parklawn Drive, Rockville, MD 20852, USA.

V. N. Gladyshev and T. C. Stadtman, Laboratory of Biochemistry, National Heart, Lung, and Blood Institute, NIH, 9000 Rockville Pike, Bethesda, MD 20892, USA.

S. V. Khangulov, Department of Chemistry, Hoyt Laboratory, Princeton University, Princeton, NJ 08544, USA.

\*Present address: Basic Research Laboratory, National Cancer Institute, NIH, 9000 Rockville Pike, Bethesda, MD 20892, USA.

†To whom correspondence should be addressed.



being stabilized and oriented by hydrogen bonding through a carbonyl oxygen of formate to both Arg<sup>333</sup> and the amide nitrogen of His<sup>141</sup> (Fig. 5). The subsequent oxidation of formate to carbon dioxide and the transfer of two electrons to the Mo center (Fig. 5) may occur either by a direct two-electron transfer through the oxygen of formate to Mo or by a direct hydride transfer to Mo. Upon Mo reduction, the  $\alpha$  proton of formate is released to the nearby His<sup>141</sup> through protonation of SeCys<sup>140</sup>. The involvement of a histidine residue is consistent with known pH dependencies in the catalytic activity of both the SeCys<sup>140</sup>  $\rightarrow$  Cys<sup>140</sup> mutant and wild-type FDH<sub>H</sub> (13), and the protonation of His<sup>141</sup> by the  $\alpha$  proton of formate is supported by electron paramagnetic resonance (EPR) observations (14). The next step is to shuttle electrons from the Mo(IV) to a downstream electron acceptor through the

Fe<sub>4</sub>S<sub>4</sub> cluster. As the first electron is transferred through Lys<sup>44</sup> to the Fe<sub>4</sub>S<sub>4</sub> cluster, it produces an intermediate [Mo(V), Fe<sub>4</sub>S<sub>4</sub>(red)] that is easily observed in EPR experiments (14). Meanwhile, the transfer of a formate-derived proton to His<sup>141</sup> will lead to hydrogen bond formation between the imidazole of His<sup>141</sup> and the selenium of SeCys<sup>140</sup> while the selenium is coordinated to Mo(V) (15). Although the nature of the in vivo electron acceptor for FDH<sub>H</sub> remains unknown, the reoxidation of the Fe<sub>4</sub>S<sub>4</sub> can be achieved with benzyl viologen, a one-electron acceptor. Once the Fe<sub>4</sub>S<sub>4</sub> cluster is reoxidized, a second electron can be transferred from Mo(V) to the Fe<sub>4</sub>S<sub>4</sub> cluster and the enzyme returns to its initial state after the second oxidation of the Fe<sub>4</sub>S<sub>4</sub> cluster. The oxidation of Mo(V) to Mo(VI) would cause the hydrogen bond between SeCys<sup>140</sup> and His<sup>141</sup> to break, thereby re-

leasing the proton of His<sup>141</sup> to solvent.

A common feature among many MPT-containing enzymes is the coupling of the redox state of Mo with the substrate oxidation-reduction process. In FDH<sub>H</sub>, the reduction of Mo(VI) to Mo(IV) profoundly affects the Mo coordination geometry and thus the conformation of MPTs. Such changes, which are also observed in model compounds (16), may represent a general feature associated with MPT-dependent Mo- and W-containing enzymes. In contrast, the incorporation of a SeCys in FDH<sub>H</sub>, as compared with incorporation of a Cys or Ser in other di(MPT)-dependent enzymes, appears to correlate with the usage of a hydroxyl ligand as opposed to sulfido or oxo ligands to Mo (7, 17, 18). This is also evident in extended x-ray absorption fine structure (EXAFS) studies of FDH<sub>H</sub> where a terminal oxo ligand to Mo is observed in a SeCys<sup>140</sup>  $\rightarrow$  Cys<sup>140</sup> mutant but not in wild-type FDH<sub>H</sub> (19). This mutation results in a much lower initial rate of substrate oxidation, 1/300 that of the wild type (13). Thus, the choice of a SeCys, Cys, or Ser ligand to Mo may serve to fine-tune the coordination of a particular cis-ligand and hence set the substrate preference. This suggests a new role of selenium in biology, involving ligation to a metal and proton transfer during catalysis.

The combination of the MPT redox center, SeCys<sup>140</sup>, and the Fe<sub>4</sub>S<sub>4</sub> cluster, each precisely positioned, results in an enzyme that not only catalyzes the oxidation of formate but also effectively couples the oxidation-reduction to an electron acceptor in the formate hydrogen lyase complex. This suggests that the MPT moiety, in addition to providing a structural framework for Mo coordination, also functions as part of an electron transfer path and potentially as an electron sink.

REFERENCES AND NOTES

- G. Sawers, *Antonie Leeuwenhoek* **66**, 57 (1994).
- M. J. Axley, D. A. Grahame, T. C. Stadtman, *J. Biol. Chem.* **265**, 18213 (1990).
- M. J. Axley and D. A. Grahame, *ibid.* **266**, 13731 (1991).
- V. N. Gladyshev, S. V. Khangulov, M. J. Axley, T. C. Stadtman, *Proc. Natl. Acad. Sci. U.S.A.* **91**, 7708 (1994).
- M. J. Romão *et al.*, *Science* **270**, 1170 (1995).
- M. K. Chan, S. Mukund, A. Kletzin, M. W. W. Adams, D. C. Rees, *ibid.* **267**, 1463 (1995).
- H. Schindelin, C. Kisker, J. Hilton, K. V. Rajagopalan, D. C. Rees, *ibid.* **272**, 1615 (1996). The overall fold of *Rhodobacter sphaeroides* DMSO reductase is similar to that of FDH<sub>H</sub>.
- R. Huber *et al.*, *Proc. Natl. Acad. Sci. U.S.A.* **93**, 8846 (1996).
- T. C. Stadtman, *Annu. Rev. Biochem.* **65**, 83 (1996); R. S. Pilato and E. I. Stiefel, in *Bioinorganic Catalysis*, J. Reedijk, Ed. (Dekker, New York, 1993), chap. 6.
- A. M. Lesk, *Curr. Opin. Struct. Biol.* **5**, 775 (1995); G. E. Schulz, *ibid.* **2**, 61 (1992).
- Sequences were obtained from the SWISS-PROT protein sequence data bank [A. Bairoch and B. Boeckmann, *Nucleic Acids Res.* **20**, 2019 (1992)] (accession numbers p07658, p06131, 032176, p24183, and

**Table 1.** Data collection, phasing, and refinement statistics for FDH<sub>H</sub> structure determination. Purification, crystallization, and cryofreezing of reduced FDH<sub>H</sub> crystals [Mo(IV), Fe<sub>4</sub>S<sub>4</sub>(red)] were performed in a nitrogen atmosphere at <1 ppm of oxygen as described (20). Crystals belong to the tetragonal space group P4<sub>1</sub>2<sub>1</sub>2 with cell dimensions of a = b = 146.3 Å and c = 82.3 Å containing one monomer in the asymmetric unit. Crystals of FDH<sub>H</sub> in the [Mo(VI), Fe<sub>4</sub>S<sub>4</sub>(ox)] state (10) were obtained by serially washing crystals in a formate-free solution and then soaking crystals in 10 mM benzyl viologen for 30 min before freezing. Crystals of nitrite-inhibited FDH<sub>H</sub> were obtained by adding 30 mM sodium nitrite to the benzyl viologen solution during oxidation. Diffraction data were processed with DENZO and SCALEPACK (21) or R-AXIS software (22) and scaled with CCP4 programs (23). MIR phases from five derivatives [K<sub>2</sub>PtCl<sub>4</sub>, Sm(OAc)<sub>3</sub>, AuCN, TMLA, and Pb(OAc)<sub>2</sub>] together with MAD and anomalous scattering phases (AuCN and TMLA derivatives, respectively) were refined using MLPHARE (23), combined with SIGMAA (23) and subsequently improved through solvent flattening and histogram matching using the program DM (23). The resulting electron density maps were readily interpretable. Model building and refinement were carried out with the programs O (24) and X-PLOR 3.1 (25). The refinement process used all data for which |I| > 2σ<sub>I</sub>. Values of I/σ<sub>I</sub> for the reduced, oxidized, and NO<sub>2</sub><sup>-</sup>-bound data sets were 26.1, 22.1, and 19.5, respectively. During the refinement, ligand bonds to Mo were only loosely restrained (1.0 kcal/Å) and the position of the selenium in reduced FDH<sub>H</sub> was fixed.

Data set*	Wave-length (Å)	d <sub>min</sub> (Å)	Reflections		Completeness (%)	R <sub>sym</sub> §	Sites (N)	Phasing power
			Measured	Unique				
Native 1	1.5418†	3.0	194,324	17,511	96.0	8.8	—	—
K <sub>2</sub> PtCl <sub>4</sub>	1.5418†	3.0	188,492	18,059	97.5	11.2	3	0.71
Sm(OAc) <sub>3</sub>	1.5418†	3.0	160,269	16,644	90.3	10.5	2	0.45
AuCN	1.5418†	3.0	161,232	18,353	99.6	10.1	6	0.95
TMLA	1.5418†	3.5	142,691	11,327	95.9	6.1	7	1.29
Pb(OAc) <sub>2</sub>	1.5418†	3.0	183,543	18,514	99.6	8.2	3	0.72
Oxidized	1.5418†	2.8	84,166	20,861	93.4	7.9	—	—
NO <sub>2</sub> <sup>-</sup>	1.5418†	2.9	94,068	19,946	97.7	9.0	—	—
Native 2	1.0402‡	2.3	169,244	36,025	88.0	8.5	—	—
AuCNλ1	1.0489‡	3.0	59,714	26,227	75.3	4.3	—	—
AuCNλ2	1.0402‡	3.0	59,419	26,306	75.4	4.3	8	0.64
AuCNλ3	1.0398‡	3.0	51,813	25,231	72.4	4.3	8	0.46
TMLAλ2	0.9493‡	3.0	88,083	29,933	85.7	4.0	8	1.28

FDH model	d spacings (Å)	R value	R <sub>free</sub>	Non-H atoms (N)	Solvent sites (N)	Mean B factor (Å <sup>2</sup> )	rmsd	
							Bonds (Å)	Angles (°)
Reduced	6.0 to 2.3	0.217	0.287	5541	83	28.4	0.013	1.81
Oxidized	6.0 to 2.8	0.195	0.288	5668	64	24.1	0.012	1.81
NO <sub>2</sub> <sup>-</sup> -bound	6.0 to 2.9	0.192	0.282	5671	62	24.1	0.012	1.80

\*All data sets were collected at -180°C. AuCN, K<sub>2</sub>Au(CN)<sub>2</sub>; TMLA, trimethyl lead acetate. †Data collected with an R-AXISIIc system (Molecular Structure Corporation). ‡Data collected at the X4A beamline of the National Synchrotron Light Source (NSLS), Brookhaven, NY. §R<sub>sym</sub> = 100 × ΣhΣI<sub>h</sub> - ⟨I<sub>h</sub>⟩/ΣhΣI<sub>h</sub>, where h are unique reflection indices, I<sub>h</sub> are intensities of symmetry-redundant reflections, and ⟨I<sub>h</sub>⟩ is the mean intensity. ||Phasing power is the rms value of F<sub>o</sub> divided by the rms lack-of-closure error.

- p46448) and the Protein Identification Resource (PIR) [K. E. Sidman, D. G. George, W. C. Barker, L. T. Hunt, *ibid.* **16**, 1869 (1988)] (accession number s18213).
12. The Mo-ligand distances in the reduced form of  $\text{FDH}_{\text{H}}$  are as follows:  $\text{MGD}^{\text{S01}}\text{S12}$ , 2.1 Å;  $\text{MGD}^{\text{S01}}\text{S13}$ , 2.3 Å;  $\text{MGD}^{\text{S02}}\text{S12}$ , 2.5 Å;  $\text{MGD}^{\text{S02}}\text{S13}$ , 2.3 Å; and Se, 2.5 Å. In the oxidized form of  $\text{FDH}_{\text{H}}$ , the Mo-ligand distances are as follows:  $\text{MGD}^{\text{S01}}\text{S12}$ , 2.6 Å;  $\text{MGD}^{\text{S01}}\text{S13}$ , 2.3 Å;  $\text{MGD}^{\text{S02}}\text{S12}$ , 2.4 Å;  $\text{MGD}^{\text{S02}}\text{S13}$ , 2.4 Å; Se, 2.7 Å; and OH, 2.2 Å.
  13. M. J. Axley, A. Böck, T. C. Stadtman, *Proc. Natl. Acad. Sci. U.S.A.* **88**, 8450 (1991).
  14. EPR spectroscopy provided evidence that the formate-derived proton is located in the vicinity of the Mo(V) center and is slowly exchangeable with water; the proton-accepting group is weakly involved in the electronic ground state of the Mo(V) center and is not a direct ligand to Mo (S. V. Khangulov, V. N. Gladyshev, T. C. Stadtman, in preparation).
  15. NMR studies of a  $\text{SeCys}^{221}$  derivative of subtilisin suggest the presence of a hydrogen bond between the protonated  $\text{N}\epsilon 2$  of  $\text{His}^{64}$  and the selenium of  $\text{SeCys}^{221}$  [K. L. House, A. R. Garber, R. B. Dunlap, J. D. Odom, D. Hilvert, *Biochemistry* **32**, 3468 (1993)].
  16. S. K. Das, D. Biswas, R. Maiti, S. Sarkar, *J. Am. Chem. Soc.* **118**, 1387 (1996).
  17. G. N. George, J. Hilton, K. V. Rajagopalan, *ibid.*, p. 1113.
  18. M. J. Barber, H. L. May, J. G. Ferry, *Biochemistry* **25**, 8150 (1986).
  19. J. Dong *et al.*, in preparation.
  20. V. N. Gladyshev *et al.*, *J. Biol. Chem.* **271**, 8095 (1996). The results of EPR studies of reduced and oxidized  $\text{FDH}_{\text{H}}$  crystals are consistent with the presence of a  $[\text{Mo}(\text{IV}), \text{Fe}_4\text{S}_4(\text{reduced})]$  state and a  $[\text{Mo}(\text{VI}), \text{Fe}_4\text{S}_4(\text{oxidized})]$  state, respectively.
  21. Z. Otwinowski, in *Proceedings of the CCP4 Study Weekend: Data Collection and Processing*, L. Sawyer, N. Isaacs, S. Bailey, Eds. (SERC Daresbury Laboratory, Warrington, UK, 1993), pp. 56–62.
  22. *R-AxisIIc Data Processing Software Version 2.1 Instruction Manual* (Rigaku Corp., 1994).
  23. *CCP4: A Suite of Programs for Protein Crystallography* (SERC Collaborative Computing Project No. 4, Daresbury Laboratory, Warrington, UK, 1979).
  24. T. A. Jones, J.-Y. Zou, S. W. Cowan, M. Kjeldgaard, *Acta Crystallogr. A* **47**, 110 (1991).
  25. A. T. Brünger, *X-PLOR Version 3.1, a System for X-ray Crystallography and NMR* (Yale Univ. Press, New Haven, CT, 1992).
  26. K. Kraulis, *J. Appl. Crystallogr.* **24**, 946 (1991); D. J. Bacon and W. F. Anderson, *J. Mol. Graphics* **6**, 219 (1988); E. A. Merritt and M. E. P. Murphy, *Acta Crystallogr.* **D50**, 869 (1994).
  27. S. V. Evans, *J. Mol. Graphics* **11**, 134 (1993).
  28. We thank D. A. Grahame for use of the anaerobic glove chamber and helpful discussions, C. Ogata and staff at HHMI beamline X4A, and Y. Zhang and L. Hannick for help in the synchrotron data collection.
- 2 August 1996; accepted 14 January 1997